

## Article

# Chromaticity of *Gromwell*, *Cape jasmine* Dyeing, and Effects of Zinc Oxide/Polyphenol Treatment with Copper Mordanting for UV Protection

Hye Jin Kim <sup>1,2,3</sup> 

<sup>1</sup> Graduate School of Design, Ewha Womans University, Seoul 03760, Republic of Korea; vodratti@gmail.com; Tel.: +82-(0)10-4408-9361

<sup>2</sup> Department of Fashion Industry, Ewha Womans University, Seoul 03760, Republic of Korea

<sup>3</sup> NewM Distance Lifelong Education Center, Seoul 07299, Republic of Korea

**Abstract:** To protect skin from harmful ultraviolet (UV) radiation, there has been a resurgence in the use of natural dyes with metal mordants to reduce contamination by advanced chemicals. This study achieved natural dyeing in violet and yellow colors from *Gromwell red* roots and *Cape jasmine* seeds for UV-protective materials. The dyed fabrics were subjected to zinc oxide (ZnO) and polyphenol treatments, as well as copper post-mordanting. The SEM, TEM, and XRD tests showed that the ZnO nanoparticles, with hexagonal crystal structures, stuck to the fiber surfaces, and twisted strands resulted in the K/S reduction. First, this study found that the untreated cotton in violet, despite the highest K/S, faded the most intensely when exposed to UV. The color variation of untreated polyester was narrow, with little change in L, a\*, and K/S. The color change of yellow-dyed samples treated with ZnO/polyphenol was not considerable in yellowness (b\*: 28.838), while the violet fabrics displayed a significant decrease in K/S and an increase in b\*. The combination of ZnO and polyphenol treatment improved UV absorption at 350 to 250 nm. Among the Cu-mordanted fabrics after ZnO/phenols treatment, the violet cotton turned reddish from blueish (negative to positive b\*), with a hue change of 316° to 59° and the highest ΔE (25.90 ± 4.34) after UV exposure. In this study, the combination of ZnO/polyphenol with Cu-mordants allowed the *Cape jasmine*-dyed polyester to achieve a minimum ΔE as well as to keep its chroma and hue after UV exposure.



check for updates

**Citation:** Kim, H.J. Chromaticity of *Gromwell*, *Cape jasmine* Dyeing, and Effects of Zinc Oxide/Polyphenol Treatment with Copper Mordanting for UV Protection. *Colorants* **2024**, *3*, 175–198. <https://doi.org/10.3390/colorants3030013>

Academic Editor: Anthony Harriman

Received: 1 April 2024

Revised: 1 June 2024

Accepted: 12 June 2024

Published: 24 June 2024



**Copyright:** © 2024 by the author. Licensee MDPI, Basel, Switzerland. This article is an open access article distributed under the terms and conditions of the Creative Commons Attribution (CC BY) license (<https://creativecommons.org/licenses/by/4.0/>).

**Keywords:** dye; xanthophyll; carotenoid; zinc oxide (ZnO); phenol; mordant; copper; K/S

## 1. Introduction

Since the global ozone crisis, ultraviolet (UV) radiation exposure has posed the threat of skin aging, inflammation, and severe damage to collagen, hyaluronic acid, and protein [1–4]. In a highly developed chemical industry, skin protection by covering functional fabrics results from the control of UV exposure by absorbing, transmitting, and reflecting UV light. For the functionalization of light transmission, a wide range of colorants are inserted onto the UV protective fabric surface, viz., dyeing. When the colorants result in stabilizing effects, the dyed fabrics are able to shield UV rays from 290 to 400 nm wavelengths. To strengthen those UV-absorbing or -shielding abilities, the protective fabrics also require additives such as titanium dioxide and zinc oxide.

Several researchers have studied how to adsorb zinc oxide (ZnO) nanoparticles onto cotton fabrics. The potential characteristics of ZnO are appropriate for UV protective materials, such as easy processibility, cost accessibility, biocompatibility, great electron mobility with high excitation binding energy, air-thermal stability, intensive photocatalytic ability, corrosion stability, and solar-UV absorption ability [5–9]. Belay et al. increased the UV protection factor (UPF) of cotton fabrics coated with ZnO nanoparticles via in situ deposition, compared with the precipitation method [10]. The UV absorption wavelength of ZnO stands out at 368 nm, equivalent to the band gap at 3.37 eV [11]. For optimal

UV protection, it is adequate for sun-blocking materials to cover the wide range of UV absorption, including UVA and UVB.

With the aforementioned excellence of ZnO, another UV protective material is also required to strengthen the absorption range of ZnO. Several researchers have recently discovered organic UV absorbers from plant extracts for marine organisms, namely, algae [12–17]. Regardless of its non-toxicity, mycosporine and its derivatives are expensive for practical use, compared with phenolic compounds from natural plant extracts. Polyphenols, one of the typical phytochemicals, can provide skin photoprotection [2,4]. Tannins of the polyphenols are mostly contained in berries, pomegranates, and green tea leaves [4,12]. The tannins from phenolic compounds can also be used as antioxidants. He et al. used polyphenols to scavenge free radicals from the hydroxyl groups of polyphenols, thereby inhibiting the generation of radicals and the polymerization of photosensitive ink via the formation of quinones [18]. However, polyphenolic compounds are known to discolor and decolorize their applied fibers and textiles, resulting in poor color fastness to light. Overall, the possibility of discoloration by the polyphenols is controversial; hence, other factors should be considered, such as photodegradation in the manufacturing, storage, and usage.

As mentioned above, photodegradation can be classified into both internal material attributes and external environmental factors. Groeneveld et al. distinguished between the internal factors, such as the inherent characteristics of colorants, photocatalysts, and textile substrates, and the external factors, such as light irradiation, oxygen, temperature [19]. When the concentration of oxygen, one of the external factors, is high in aerobic environments, the rate of photodegradation can accelerate because the oxidation causes decolorization by decomposing chromophores [20]. On the other hand, the hydrogen ion exponent (pH) of a dyeing solution, one of the internal factors, is a paramount cause of color change through photocatalyst oxidation. Not only the pH dye solution but also the type of textile substrate are of vital importance. Nylon, wool, silk, and leather can easily be discolored or yellowed due to the chain scission of amino groups after being exposed to UV, nitrogen dioxide, ozone, moisture, and heat. Despite the weakness of proteinaceous fibers to photodegradation, acid dyeing enables wool to prevent discoloration or decolorization by neutralizing negative charges and forming cystine bonds on the woolen surface. In addition, the type of chromophores excited in colorants differentiates the photochemical mechanisms between visible and UV regions.

To minimize the decolorization affected by the factors mentioned above, it is necessary to understand photochemical mechanisms, which are dependent on the photon absorption of colorants or dye molecules. Three photochemical mechanisms can be explained through direct or indirect photochemical reactions by photosensitizers, photocatalysts, and hydrogen as follows: photoisomerization, photooxidation, and photoreduction [21]. Photoisomerization arises from the structural transformation of photocatalytic chromophores—for instance, chlorophylls glowing with an autumn color into red, yellow, or brown. Trans-isomers of chromophores in natural dyes can be converted to cis-isomers when absorbing light irradiation of a short wavelength, resulting in the discoloration of the dyed textiles [22]. Naphthoquinone, one of the quinonoid compounds, comprises many isomers, such as alkannin, lawsone, juglone, lapachol, plumbargin, and shikonin [23,24]. La and Giusti investigated the photochromism of delphinidins in anthocyanin dyes between trans- and cis-acylated isomers that were induced by visible UV light reversibly [25]. Carotenoids, one of the photoprotective dyes, are generated by the cis-trans isomerization of polar lutein and zeaxanthin, whereas the carotenoids turn into xanthophylls or  $\beta$ -cryptoxanthins due to the oxidation of the 3-hydroxy- $\beta$ -end group of the xanthophyll [26]. The chromatic structures of chromophore groups can also be transformed by benzoyl peroxide, which causes the discoloration of their applied textiles. According to Rafiq et al., photooxidation occurs when photocatalytic dyes produce holes and electrons in excited states where photon absorption is higher than the bandgap energy of the photocatalytic dyes [27]. The chromophoric group photooxidates polyolefins due to the generation of reactive oxygen species and hydrogen peroxide, breaks down into hydroxyl and alkoxy radicals under

Norrish and cage reactions, and finally terminates recombination in stabilized states [28]. On the other hand, photoreduction occurs when excited electrons, such as ketones, react with hydrogen from other molecular materials. The difference between photooxidation and photoreduction can be distinguished by the area of decolorization; for example, the only faded area of photo-reduced fabrics is where they were exposed to light, whereas the area covered with wrinkles or screened did not fade. In conclusion, discoloration through the photochemical reactions can be prevented by dyeing fabrics with photo-protective colorants with monochromaticity, by coordinating with metallic compounds, and by treating antioxidants and UV absorbers or blockers to apply the photo mechanisms.

To avoid photodegradation, metal-polyphenolic chelating compounds can benefit from both metal cations donating electrons, and tannin against photooxidation. Catechol or gallol groups in the polyphenols play a role as ligands to chelate with metals, metal oxides, or carbon nanomaterials [13,14]. Feng et al. stated that catechol's exceptional capacity to adsorb, attach, and bind to a variety of substrates, from hydrophilic to hydrophobic or from organic to inorganic surfaces, allows it to coordinate with metals such as Fe, Cu, Zn, and Al [14]. Wang et al. demonstrated that the electroless deposition of ZnO and cotton surface modification could maintain high UPF mechanical properties even after 50 launderings with palladium as a catalyst and tannic acid as a linking agent [29]. The improvement in UV protection could be attributed to the fact that a large amount of ZnO and polyphenols from plant extracts were adsorbed onto inherently hollow cotton fibers, leading to UV absorption. The metal-polyphenolic coordination materials can result in synergistic effects on antioxidants and antiaging against the broad ranges of UV light, with tannins acting as organic UV absorbers and ZnO acting as inorganic UV blockers [3].

In this study, the inheritance of natural dyeing and metallic mordanting was aimed at overcoming low resistance to light and to washing for the application to UV-protective textiles. Two types of natural dyes in violet and yellow colors were extracted for cotton and polyester fabrics from naphthoquinone and  $\beta$ -carotenoid chromophores from *Gromwell* red-roots and *Cape jasmine* seeds. To improve UV light protection, the treatments of zinc oxide and polyphenols were studied through the UV-Vis reflectance analyses in comparison with color differences ( $\Delta E$ ) between untreated and treated fabrics after UV exposure. The final purpose of the study was to examine the chromaticity of four metallic mordants, especially Cu-post mordanting, using CIELAB  $b^*$  values and color depth (K/S).

## 2. Materials and Methods

### 2.1. Materials

In this study, violet and yellow in complementary colors were chosen to find the effects of mordanting, UV protective treatment, and exposure to UVC rays on the chromatic variation of dyed fabrics. As natural dyes, this work selected *Gromwell* roots (GWR), or *Lithospermum erythrorhizon* pellets, and *Cape jasmine* seeds (CJS), or *Gardenia jasminoides*. Both dyes were purchased at the Boncho Myeong-ga Industry-Daejeon University Cooperation Foundation. The extraction of GWR-Violet and CJS-Yellow dyes was conducted using anhydrous ethanol (purity 99%, Shinhwan International Co., Ltd., Seoul, Republic of Korea) and tertiary purified water (Joylife Corp., Gimhae, Republic of Korea), respectively. To facilitate the extraction of GWR-Violet dyes, 99% acetic acid (Samyang Ltd., Ansan, Republic of Korea) was diluted. Zinc oxide (ZnO) and tannin as polyphenolic compounds, which were derived from gallnut (*Quercus infectoria*), were selected to increase UV absorption in this research. The zinc oxide powder was obtained from Gooworl Corp. (Daegu, Republic of Korea) and the gallnut powder was obtained from Yeongcheon Herb Medicine Farming Association Co., Ltd. (Yeongcheon, Republic of Korea). The ZnO particles were dispersed in tertiary purified water and dimethyl sulfoxide (DMSO) (purity 99.8%, KisanBio, Seoul, Republic of Korea).

To investigate the influence of post-mordanting on color variation, four mordants were used: aluminum potassium sulfate ( $KAl(SO_4)_2$ ), copper acetate ( $Cu(OAc)_2$ ), tin chloride ( $SnCl_2$ ), and iron sulfate ( $FeSO_4$ ). The aluminum potassium sulfate and iron sulfate were

supplied from Sinsegi Science Corp., Seoul, Republic of Korea. Common copper plates were dissolved in diluted acetic acid (5 M) to make a copper acetate solution. A tin chloride solution was prepared by dissolving tin powder (96.5% Sn, 500 mesh) in 36.5% hydrochloric acid (Junsei Chemical Ltd., Tokyo, Japan). The tin powder was obtained from Juju Industry, Bucheon, Republic of Korea, and its size ranged from 25  $\mu\text{m}$  to 80  $\mu\text{m}$ .

## 2.2. Extraction of Natural Dyes and Preparation of Mordants

The first step was to extract the violet dyes from red-roots of *Gromwell* (GWR), *Lithospermum murasaki Siebold*, as shown in Figure 1a,b. In total, 60 g of GWR pellets were mixed with 500 mL of ethanol. After diluting 50 mL of 5 M acetic acid with tertiary filtered water, it was added to the GWR/ethanol solution. The solution was kept at room temperature for 72 h with the container lid closed to prevent ethanol from evaporating. For the extraction of yellow dyes, 50 g of dried seeds from *Cape jasmine* (CJS) plants, *Gardenia jasminoides J.Ellis*, as seen in Figure 1c,d, was soaked in 500 mL of water at 40 °C for 24 h. After 24 h, the first CJS-Yellow extract was filtered through a piece of muslin cloth into an Erlenmeyer flask and then left with its neck wrapped in aluminum foil. The residue seeds were extracted in another 500 mL of water in the second round, followed by the same procedure as detailed above. After another 24 h, the second CJS extract was added to the first dye solution for homogenization.



**Figure 1.** Photographs of (a) red-root *Gromwell* plants, (b) dyes from the *Gromwell*, (c) *Cape jasmine* plants, and (d) dyes from the seeds. Photographs (a,c); Reproduced with permission from [National Species Knowledge Information System]. Copyright Sooyoung Jeong, Korea National Arboretum, 2016 (a), 2011 (c). Copyright is prohibited from unauthorized reproduction or distribution, available from at [www.nature.go.kr](http://www.nature.go.kr), accessed on 30 May 2024 [30].

The second step was to prepare the photo-absorbers, zinc oxide powder, and crushed gallnut for UV protective treatment. The ZnO (6% o.w.f.) was dispersed in a 500 mL mixture of 350 mL of ethanol and 150 mL of purified water for the first treatment. For the second treatment, another 12% o.w.f. of ZnO powder was in 50 mL of DMSO. Both ZnO dispersed solutions were magnetically stirred for 60 min, followed by ultrasonication for five mins. To extract pyrogallol acid from polyphenolic tannin, 25 g of the gallnut was ground in a mortar with a pestle, and the residual dust was removed. A total of 125 mL of purified

water was poured into the ground gallnut and then boiled for one hour. After extracting the boiled solution, another 125 mL of water was added to the filtered gallnut, which was then boiled for another hour. Finally, all of the extracts were gathered into one container.

The next step was to dissolve metallic salts and thin metal pellets in each solvent for pre- and post-mordanting. The aluminum potassium sulfate (8% o.w.f.) and iron sulfate (2% o.w.f.) powders were respectively stirred in 1 L of distilled water for 60 min and kept at room temperature to stabilize for another 60 min. The copper plates were sliced into pieces ranging in size from 3 mm to 5 mm. Then, 10 g of copper pellets was dissolved in a solution of 25 mL of purified water and 25 g of 5 M acetic acid. To accelerate the dissolving reaction, 9.7 M hydroperoxide was carefully added dropwise to the copper acetate solution and left at room temperature for 48 h. The copper acetate solution turned blue, and the residual Cu pieces were filtered from the blue solution. For the preparation of tin chloride mordants, 2.457 g of tin power (500 mesh) was dissolved in 10 mL of 37% HCl in a three-neck reaction flask with rubber septa sealing and a magnet and stirred at 75 °C. After 2 h, 2 mL of purified water was added to the solution and then left on the hot plate without stirring for 12 h. Finally, the tin chloride solution was cooled to room temperature for another 12 h.

### 2.3. Natural Dyeing and Mordanting

In this study, two sets of cotton and polyester fabrics were dyed. Polyester nanofilament and organic cotton yarns were supplied by Kolon Fashion Material Ltd. (Gwacheon, Republic of Korea) and Hanjoong Union Ltd. (Seoul, Republic of Korea), respectively. The combed cotton for warp yarns was provided by Dong-A TOL Ltd. (Daegu, Republic of Korea), where the weaving sampling was processed in this work.

As listed in Table 1, the first set for violet-dyeing was two types of twill-woven fabrics, made of (a) 100% cotton combed yarn (84.7 Nm) for both warp and weft and (b) the same cotton yarn for warp/polyester nanofilaments (8.33 tex) for weft. The second set for yellow-dyeing also included two types of satin-woven fabrics, comprising (c) 100% organic cotton (101.6 Nm) for weft with 100% cotton combed yarn (84.7 Nm) for warp and (d) the same cotton warp with polyester (8.33 tex). Each density (warp/weft) was as follows: (a) 172.5/110.4, (b) 104.0/104.0, (c) 145.7/122.8, and (d) 145.7/122.4 (unit: thds/inch). All fabrics were cut to 10 cm by 10 cm in size. Prior to dyeing, the cut fabrics were refined in tertiary purified water. After that, those were squeezed and dried at room temperature. For pre-mordanting, the fabrics were immersed in a  $KAl(SO_4)_2$  solution for 20 min.

For dyeing in violet, first of all, 2 L of preheated water at 40 °C was poured into 100 mL of the *Gromwell* root extract. After being pre-mordanted, 15 g of wet twill fabrics was soaked in the extract. To prevent dye aggregation and bubble formation, the fabrics were turned over front and back and kept without floating. After 40 min, the violet-dyed fabrics were taken out of the extract, soaked in clean water for 10 min, and rinsed in flowing water. Finally, they were squeezed, dried in an oven at 35 °C, and ironed for wrinkle removal. This process is one cycle of violet dyeing. Before the second cycle, the dried fabrics were Al-mordanted repeatedly to strengthen color depth. As for yellow-dyeing, 27 g of wet satin fabrics were prepared as explained above. The fabrics were immersed in the *Cape jasmine* extract in a bath ratio of 1:20 at 70 °C for 30 min. The other processes underwent the same process as for violet dyeing.

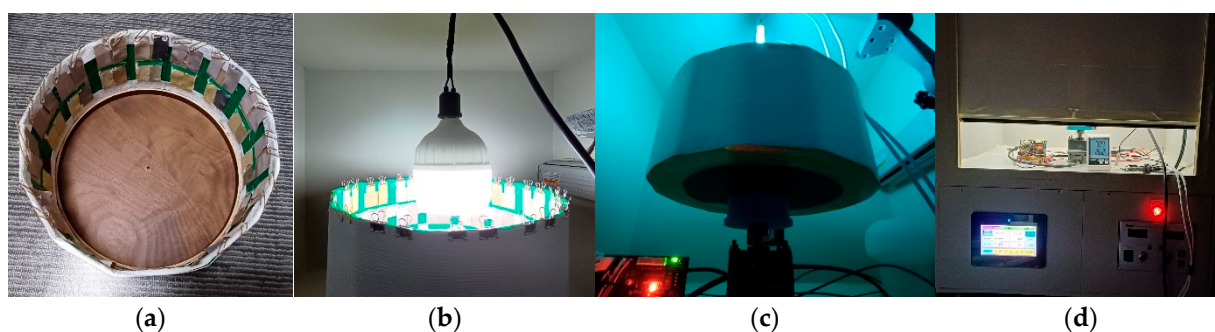
The first UV protective treatment began between the third and fourth dyeing cycles. First, the dyed fabrics were immersed in the dispersion of ZnO in ethanol or water for 30 min, rinsed, squeezed, dried, and ironed, as aforementioned. For the second UV treatment, the four-time-dyed fabrics were soaked in the dispersion of ZnO in DMSO for 20 min, and the other procedure was identical to the previous one. As for the polyphenol treatment, half pieces of the ZnO-treated fabrics were put in the gallnut extract at 40 °C and then heated to 70 °C for 30 min. The ZnO and phenol were treated twice, respectively.

Post-mordanting started after the fifth dyeing cycle, except Al- pre-mordanting. First, 50 mL of copper acetate was poured into 1 L of purified water, and one-fourth of the dyed

fabrics was sunk into the diluted solution for 10 min. The Cu-mordanted fabrics were squeezed, soaked, rinsed in water, dried, and ironed. Then, Cu-post-mordanting was repeated for another 10 min. As for Sn-post-mordanting, 25 mL of tin chloride was diluted in 500 mL of distilled water. The other steps were the same as those of Cu-mordanting. The procedure for Fe-mordanting with iron sulfate powder was the same as that detailed above.

#### 2.4. Exposure to UV-C, D65 Lamps, and Color Fastness to Light and Washing

To evaluate the fadedness of dyed fabrics by UV or artificial lamps, a new design of a UV testing apparatus was invented for this research. In Figure 2, the apparatus consisted of illuminating sources, a rotating cylinder holding samples, a motor and its controller, and a chamber to block UV-C light. Figure 2a shows the open tetradecagonal cylinder of 17 cm in diameter with 14 pieces (w: 7 cm × h: 15 cm) to hold testing fabrics. The samples were cut at 2 cm × 5 cm. A couple of sample pieces were held inside with clips and tapes, as shown in Figure 2b. A Xenon lamp was replaced with a 6500K LED lamp (60 Hz, 40 W, Yuzhong Gaohong Ltd., Hangzhou, China) and two UV-C lamps (8W, Osram, Munich, Germany), Phillips, Eindhoven, The Netherlands. The UV lamps were stuck with their backs to each other and hung on the chamber ceiling. The brushless DC motor (K8XH50N2, GGM, Bucheon, Republic of Korea) was rotating at a rate of 10.5 rpm during the testing (Figure 2c). The motor was connected to the PLC controller and touch screen, as seen in Figure 2d. The testing samples were exposed to UV lamps twice per 10 h and to the D65 light for 20 h. The total exposure time was 40 h under the data-logged chamber condition at 30.3 °C and a 27.8% RH average.



**Figure 2.** Photographs of the UV light exposure apparatus: (a) a tetradecagonal holder; (b) a rotating apparatus with a 6500K lamp; (c) a rotating DC motor with UV-C lamps; and (d) a PLC controller with a touch screen in the chamber.

Color fastness to light was conducted at an A1 exposure cycle ( $45 \pm 3$  °C) for 20 h under the standard ISO 105-B02:2014 [31]. Then, the color fadedness of the samples exposed to the Xenon arc lamp was compared to that of the blue wool references. The color fastness to washing followed the standard ISO 105-C06: 2010 [32] at  $40 \pm 2$  °C for 30 min with European Color fastness Establishment detergent. Color staining tests were also implemented with two sets of test fabrics: cotton and wool/polyester.

#### 2.5. Characterization and Chromatic Analyses

To investigate the components and functional groups of the natural dyes, attenuated Fourier transform infrared (ATR-FTIR) spectrometry (Invenio-R, Bruker Corp., Billerica, MA, USA) was used. The FTIR measurement ranged from  $400 \text{ cm}^{-1}$  to  $4000 \text{ cm}^{-1}$ , at a resolution of 4.0. The spectral analyses were conducted using KnowItAll Informatic System 2024 (Wiley Science Solutions) and the OPUS (Bruker Optik GmbH, Ettlingen, Germany, v.8.7) program.

To confirm the ZnO crystalline structure and the size of the ZnO particles, the D/Max-2200/VPC (Rigaku Corp., Tokyo, Japan) X-ray diffractometer (XRD) was employed. The measurement parameters of X-ray diffraction were set at 40 kV/30 mA, with a scanning

range of  $2\theta$  from  $25^\circ$  to  $85^\circ$ . The XRD peaks were analyzed with reference cards from the Joint Committee on Powder Diffraction Standards (JCPDS) database, and the ZnO size was estimated through the Debye–Scherrer equation using Origin Pro 2024 software (Origin-Lab, Northampton, MA, USA). The average ZnO particle size was calculated using the Debye–Scherrer equation [33]. The crystallite size ( $D_{hkl}$ ) was estimated using Equation (1):

$$D_{hkl} = \frac{\kappa\lambda}{\beta \cos \theta} \quad (1)$$

where  $\kappa$ ,  $\lambda$ ,  $\beta$ , and  $\theta$  are Scherrer's constant (normally considered as 0.9), the wavelength of the X-ray beam (the copper used in this study,  $\lambda$  1.54184 Å), the full width at half maximum (FWHM) of the peak, and Bragg's angle, respectively.

The aforementioned ZnO particles were observed through a Scanning Electron Microscope (SEM). The SEM microscopic images were obtained at 15 kV using a Mini Cube 2 (Emcrafts Co., Ltd., Hanam, Republic of Korea). The ZnO particles were dispersed in the DMSO solution; then, the dispersion was dropped on a copper TEM grid (200 mesh) with carbon lacey film. After the ZnO dispersion was dried, the TEM observation was conducted via a Field Emission Transmission Electron Microscope (FE-TEM) (Jeol Ltd., model: JEM-2100F, Tokyo, Japan).

To find the effects of various mordants and UV exposures on the color and UV absorbance of the dyed fabrics, the UV-3600i Plus (Shimadzu Corp., Kyoto, Japan) was utilized to measure UV-vis-NIR spectra with its deuterium lamp and integrating sphere attachment. The reflectance in the UV-vis spectrum was measured at an interval of 2 nm, and the light source was automatically switched at 310 nm. The reflectance ( $R$ ) was converted into color strength ( $K/S$ ) at 600 nm ( $\lambda_{\max}$  GWR-V) and at 450 nm ( $\lambda_{\max}$  CHS-Y) using the Kubelka–Munk equation Equation (2):

$$\frac{K}{S} = \frac{(1 - R)^2}{2R} \quad (2)$$

From the UV-vis spectra, the chromaticity and color difference coordination were obtained under a standard observer at  $10^\circ$  via the OriginPro 2024 program. The reflectance spectrum was converted to the colorimetric parameters  $L$ ,  $a^*$ , and  $b^*$  in CIELAB color spaces. The total color difference ( $\Delta E$ ) between a testing sample and a reference sample was summarized using Equation (3) as follows:

$$\Delta E = \sqrt{(\Delta L)^2 + (\Delta a)^2 + (\Delta b)^2} \quad (3)$$

where the  $L$ ,  $a^*$ , and  $b^*$  values indicate the color differences in lightness ( $L$ ), the amount of red/magenta (+) from green (−), and the amount of yellow (+) from blue (−) between the reference and test samples. The values of chroma ( $C$ ) and the hue angle ( $H$ ) were estimated using the following Equations (4) and (5) [34,35]:

$$C = \sqrt{a^{*2} + b^{*2}} \quad (4)$$

$$H_0 = \tan^{-1} \left( \frac{b^*}{a^*} \right) \cdot \frac{360}{2\pi} \quad H = \begin{cases} H_0 & \text{if } a^* > 0, b^* > 0 \\ H_0 + 180^\circ & \text{if } a^* < 0, b^* > 0 \\ H_0 + 180^\circ & \text{if } a^* < 0, b^* < 0 \\ H_0 + 360^\circ & \text{otherwise} \end{cases} \quad (5)$$

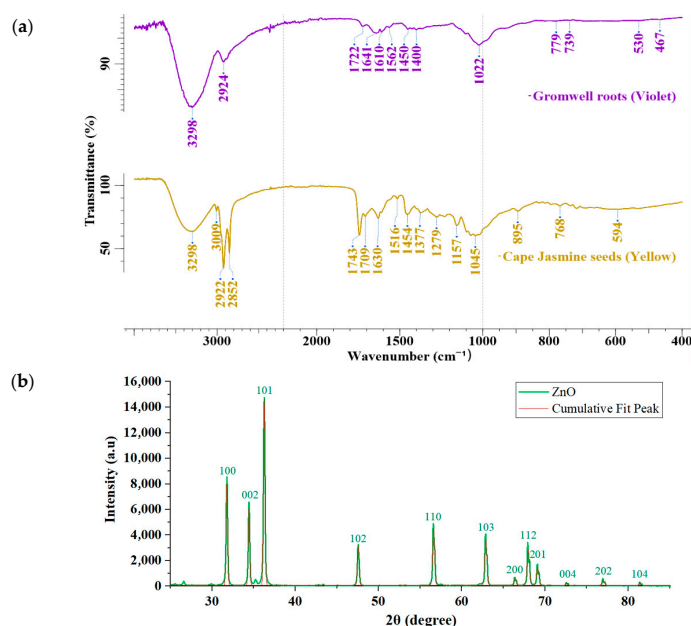
Based on the colorimetric parameters above, this study adopted the CIEDE 2000 and CMC formulae defined by the Color Measurement Committee of the Society of Dyers and Colorists for the optimum values of color difference. The weighing factors were set as follows:  $kL = 1.5$ ,  $kC = 1.9$ , and  $CMC = 2:1$  [36,37]. The values were converted through the ColorCalculator programs, which are provided by Lindbloom and Osram Inc. (Wilmington, MA, USA).

### 3. Results

#### 3.1. ATR FTIR Analyses of Natural Dyes and XRD Analyses of Zinc Oxide

Using ATR-FTIR spectra, structural investigations were carried out to investigate the auxochromic and chromophoric groups of two dyes derived from natural plants. The yellow-to-orange color hue of *Cape jasmine* seeds is derived from long conjugated double bonds of carotenoids that are categorized into carotenes and xanthophylls, with carbon and hydrogen in common and oxygen existing only in the xanthophylls [38]. As a medicinal herb due to its antioxidants, antiinflammation, and detoxification, shikonin ( $C_{16}H_{16}O_5$ ), one of the naphthoquinone compounds, imparts its violet and purple hues via its naphthalene group (with an absorption peak at approximately 490, 520, and 560 nm) [39–41].

Figure 3a identifies the IR spectroscopic results of the two natural dyes. The prominent characteristic of both dyes was the broad peak of O-H stretching vibrations at  $3298\text{ cm}^{-1}$  (GWR-Violet-dyes) and  $3329\text{ cm}^{-1}$  (CJS-Yellow-dyes). [42,43]. In addition, carboxyl groups (C=O stretching) ( $1750\text{ cm}^{-1}$  to  $1710\text{ cm}^{-1}$ ) were found in each dye spectrum [39,44]. *Cape jasmine* seeds consist of fatty acids, terpenoids, phenols, genipin, and crocin, which is a colorant belonging to carotenoids [45]. Xanthophyll is the carotenoid component with oxygen; however,  $\beta$ -carotene is another carotenoid component without oxygen. Therefore, the FTIR spectrum in Figure 3 contained oxygen; consequently, it was found that the CJS-Yellow dye was xanthophyll. This fact was also proven in reference [38,44]. Medium peaks of C-O functional groups can be seen at  $1045\text{ cm}^{-1}$  in the yellow dyes and at  $1022\text{ cm}^{-1}$  in the violet dyes. In common, each symmetric C-H stretching band from alkanes was also observed at  $2924\text{ cm}^{-1}$  (GWR-Violet-dyes) and  $2921.88\text{ cm}^{-1}$  (CJS-Yellow-dyes), respectively [39,42]. The C-H bending vibrations of GWR-Violet and CJS-Yellow dyes absorb at low wavenumbers of 779 to  $739\text{ cm}^{-1}$  and  $895\text{ cm}^{-1}$ .



**Figure 3.** (a) Attenuated FTIR spectra of *Gromwell* roots-violet dyes, *Cape jasmine* seeds-yellow dyes, and (b) XRD peaks of ZnO nanoparticles.

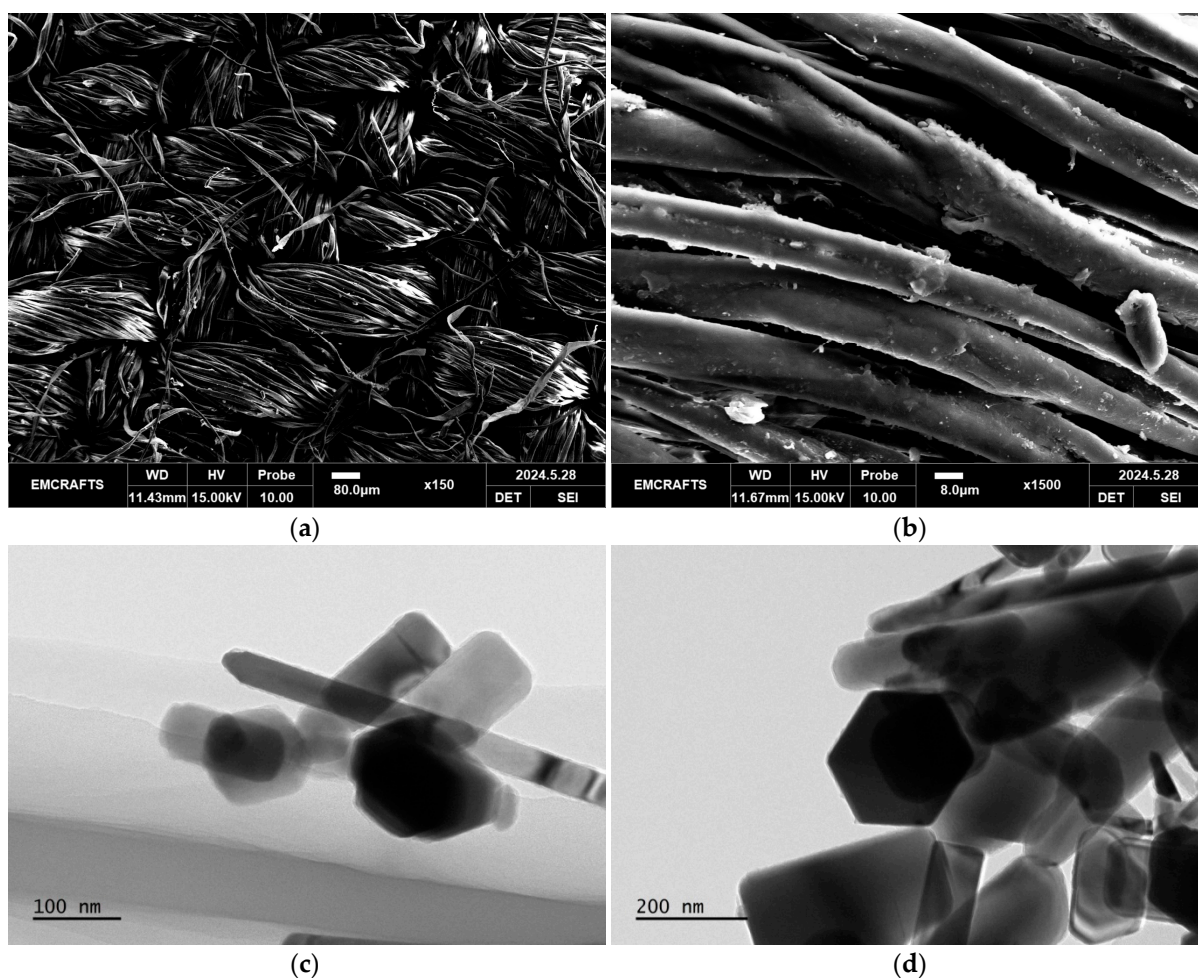
Both dyes were also characterized by an inherent peak. In the GWR-violet dyes, aromatic rings (C=C vibration) were also in naphthoquinone bands at  $1562\text{ cm}^{-1}$  [46]. The CJS-Yellow dyes revealed a weak peak at  $3009\text{ cm}^{-1}$ , which can be attributed to alkenyl C-H stretching bands. However, it was found that the violet dye and the yellow dye are respectively consistent with shikonin components from naphthoquinone and xanthophyll from  $\beta$ -carotenoid, based on the results of the FTIR spectra.

The twelve XRD peaks in Figure 3b verified the ZnO wurtzite crystalline structure, which is in conformity with the JCPDS database reference (code: 01-079-2205). The struc-



tural patterns presented their hexagonal structure from the measured peaks (planes) at  $31.76^\circ$  (100),  $31.76^\circ$  (002),  $34.42^\circ$  (101),  $36.26^\circ$  (102),  $47.54^\circ$  (110),  $56.60^\circ$  (103),  $66.36^\circ$  (200),  $67.96^\circ$  (112),  $69.08^\circ$  (201),  $72.58^\circ$  (004),  $76.96^\circ$  (202), and  $81.38^\circ$  (104). The highest peak (17,163 a.u.) was at the  $36.26^\circ$  (101) plane with an atomic spacing of 37.494 nm. With Scherrer parameters, the ZnO crystallite size was estimated from the XRD peaks after smoothing and non-linear curve fitting with the Gauss model. As a result, it was concluded that the average ZnO crystallite size was 35.36 nm, which was enough to be adsorbed on fabrics.

To validate the XRD results, the ZnO nanoparticles were observed in SEM and TEM images. Figure 4a revealed the cotton fabrics yellow-dyed with ZnO treatment at the lower magnification ( $\times 150$ ). In Figure 4b, fine particles were attached to the cotton fibers, especially in the niches of twisted strand fibers (higher magnification:  $\times 1500$ ). Figure 4c illustrates the nanoscale ZnO particles of prism shapes in DMSO dispersion for UV treatments. The range of primitive edges in the c-axis varies from 56.67 nm to 393.95 nm in length. The average edge length in the c-axis was 183.39 nm. In Figure 4d, the hexagonal basal face was clearly observed with its edge of 131.87 nm, on average, between its vertices. This length was somewhat longer than that in the XRD results. This could be because high-resolution TEM images are prone to be distorted by the interference of various diffracted/transmitted beams, the dispersion of incident beams, and the spherical/chromatic aberration of the objective lens.



**Figure 4.** SEM images of (a) cotton fabrics yellow-dyed with ZnO treatment. (b) With high magnification, TEM images of (c) ZnO wurtzite crystal structures and of (d) the hexagonal facet of the ZnO particles.

### 3.2. Coloration of Cotton and Polyester Fabrics in Violet and Yellow from Natural Dyes

In this research, two natural dyes, three types of UV protective treatment (including untreated samples), and four metallic mordants were applied to the 100% cotton and polyester weft fabrics. Tables 1 and 2 indicate the color variation of *Gromwell* roots (GWR\_V)- and *Cape jasmine* seeds (CJS\_Y)-dyed fabrics with various UV light absorbers and mordants. The Al-mordanted fabrics without any other treatments and post-mordants were categorized into 11C, 21C, 31C, 41C, 51C, and 61C of cotton weft samples and 12P, 22P, 32P, 42P, 52P, and 62P of polyester weft ones in both violet (Table 1) and yellow (Table 2) colors. The UV light-exposed fabrics were coded as “sample name\_0” to identify them before and after UV light testing.

**Table 1.** Categorization of *Gromwell*-roots dyed fabrics with various mordanting and UV protective treatments.

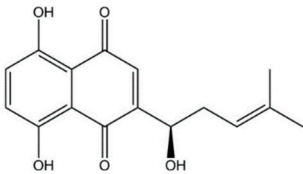

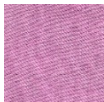
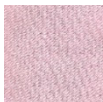



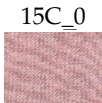
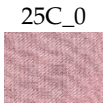
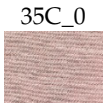





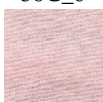



Materials	Description/Samples						Treatment
Dyes	<i>Gromwell</i> roots (Violet-dyes) [47] 						
Fabrics	Cotton-weft twill			Polyester-weft twill			
Metallic mordants	UV photo-absorber						UV light exposure
	Pristine	ZnO	ZnO/phenol	Pristine	ZnO	ZnO/phenol	
KAl(SO <sub>4</sub> ) <sub>2</sub>	11C	21C	31C	12P	22P	32P	Before
							After
Cu(OAc) <sub>2</sub>	15C	25C	35C	15P	25P	35P	Before
							After
SnCl <sub>2</sub>	16C	26C	36C	16P	26P	36P	Before
							After

Table 1. Cont.

Materials	Description/Samples						Treatment
FeSO <sub>4</sub>	17C	27C	37C	17P	27P	37P	Before
	17C_0	27C_0	37C_0	17P_0	27P_0	37P_0	

Table 2. Categorization of *Cape jasmine* seeds-dyed fabrics with various mordanting and UV protective treatments.

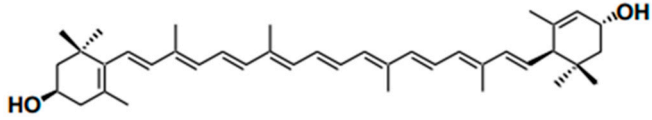
Materials	Description/Samples						Treatment
Dyes	<p><i>Cape jasmine</i> seeds (Yellow-dyes) [26]</p> 						
Fabrics	Cotton-weft satin			Polyester-weft satin			
Metallic mordants	UV photo-absorbers						UV light exposure
	Pristine	ZnO	ZnO/phenol	Pristine	ZnO	ZnO/phenol	
KAl(SO <sub>4</sub> ) <sub>2</sub>	41C	51C	61C	42P	52P	62P	Before
	41C_0	51C_0	61C_0	42P_0	52P_0	62P_0	After
Cu(OAc) <sub>2</sub>	45C	55C	65C	45P	55P	65P	Before
	45C_0	55C_0	65C_0	45P_0	55P_0	65P_0	After
SnCl <sub>2</sub>	46C	56C	66C	46P	56P	66P	Before
	46C_0	56C_0	66C_0	46P_0	56P_0	66P_0	After

Table 2. Cont.

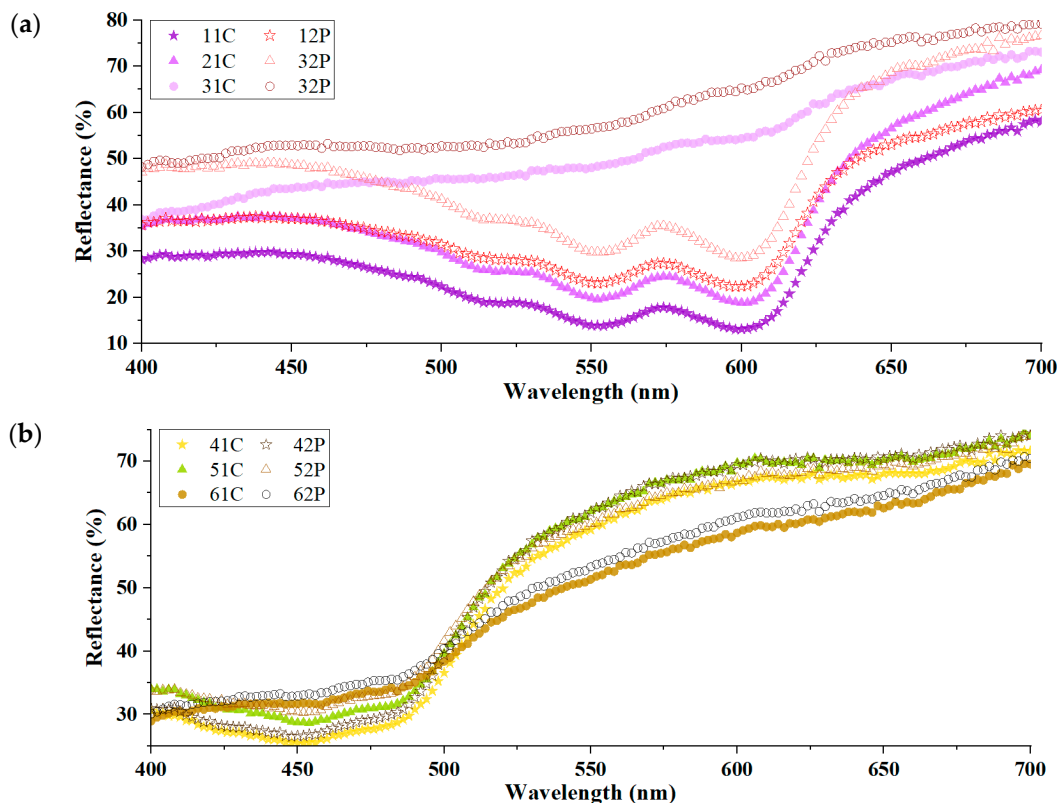
Materials	Description/Samples						Treatment
FeSO <sub>4</sub>	47C	57C	67C	47P	57P	67P	Before
	47C_0	57C_0	67C_0	47P_0	57P_0	67P_0	After

In Table 1, it was evident that the color change occurred in the fabrics treated with ZnO/polyphenols. Compared with the pristine samples, the ZnO/polyphenol-treated sample (31C to 37C) changed to become yellowish and brighter, being affected by phenolic gallnuts. The lightness values of the untreated samples (11C, 12P) were similar to those of the ZnO-treated samples (21C, 22P), or slightly increased after the sole ZnO treatment. In terms of the impacts of post-mordants, the samples 37C and 37P were distinctly darker and blackish because of iron sulfate mordanting. It was also seen that the UV light exposure caused distinguishable color changes between the unexposed violet-dyed fabrics and the ones exposed to UV light due to fadedness. In contrast, the ZnO/gallnut-treated samples did not exhibit considerable differences in fadedness.

Table 2 illustrates the color variation of *Cape jasmine* seeds (CJS-Y)-dyed fabrics. Compared to the violet-dyed ones, the yellow-dyed fabrics did not represent severe color differences between the unexposed samples (41C to 67P) and the UV-light-exposed ones (41C\_0 to 67P\_0), in contrast with the GWR-Violet-dyed fabrics. The similarity of the yellow-dyed fabrics before and after UV light exposure was higher than that of the violet-dyed ones. To take a closer look, first, the Cu-mordanted samples revealed lower lightness than the pristine ones, whereas the Sn-mordanted samples became more chromatic. It was found that Sn-mordanting made the dyed fabrics brighter and brighter (higher lightness) in both Tables 1 and 2. The highest yellow hue was observed in 46C after Sn-mordanting, in 41C after Al-mordanting, and in 45C after Cu-mordanting, and the lowest yellow hue was observed in 47C after Fe-mordanting. However, the UV-exposed samples with Sn-mordanting were clearly faded, with much higher lightness than the unexposed ones. In addition, the hue of the ZnO/polyphenol-treated samples turned reddish. Last but not least, Fe-mordanting imparted the lowest lightness and the highest color strength to the ZnO/polyphenol-treated samples, followed by the ZnO-treated ones and then the untreated ones, in the order that stood out as 47C/47P > 57C/57P > 67C/67P. This effect of iron sulfate on yellow-dyed samples, conversely, differed from that on violet-dyed ones.

### 3.3. Chromaticity of UV Absorbers and Metallic Mordants

Figure 5 demonstrates the effects of UV protective treatments on light absorbance from the reflectance spectra of the pristine samples and the treated ones. The *Gromwell* root colorants were shown to be most absorbed in the wavelength range of red to blue peaks at roughly 520, 560, and 600 nm in Figure 5a. However, the ZnO/polyphenol-treated samples (31C, 32P) did not exhibit any clear peaks, implying a loss of red and blue hues. In Figure 5b, the peak of the yellow-dyed samples appeared at approximately 450 nm, which was slightly shifted towards 420–430 nm, where the yellow color is usually absorbed. This phenomenon can be attributed to the bathochromic effect, as mentioned in other studies [23,46]. The lowest reflectance with the highest absorbance was seen in the yellow-dyed samples of 41C and 42P samples without the UV protective treatments in this study.



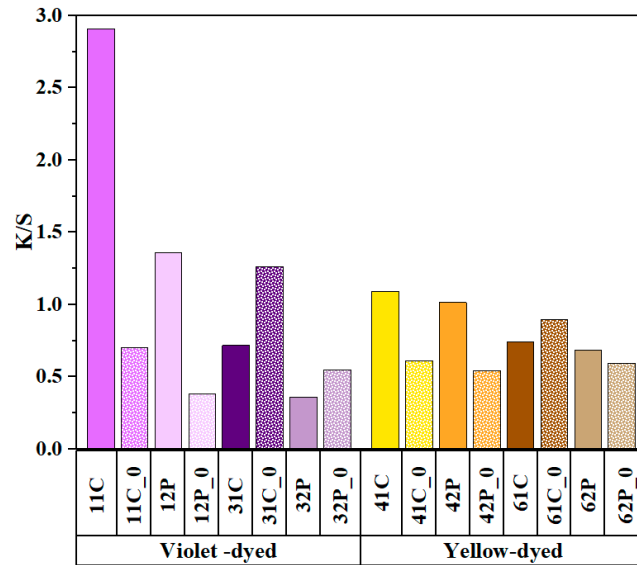
**Figure 5.** Reflective spectra of the cotton and polyester fabrics dyed with (a) shikonin and (b) xanthophyll with/without UV protective treatment.

#### 3.4. Color Depth (K/S) and Colorimetric Parameter ( $b^*$ ) with ZnO/Polyphenol Treatment after UV Exposure

In contrast to the aforementioned reflective curves, Figure 6 illustrates the CIELAB colorimetric parameter K/S values. The K/S values represent the color depth or concentration after dyeing, which were related to the molar absorption coefficient from the Beer–Lambert law and the auxochrome groups [23]. Overall, dramatic changes in colorimetric parameters were more prominent in the dyed cotton than in the dyed polyester. Another point was the order of K/S values: the pristine samples > the ZnO-treated samples > the ZnO/polyphenol-treated samples. This denotes that the reduction in K/S values corresponded to the decrease in the dye concentration by the insertion of ZnO and polyphenols. This tendency was consistently found in color dyeing in both violet and yellow.

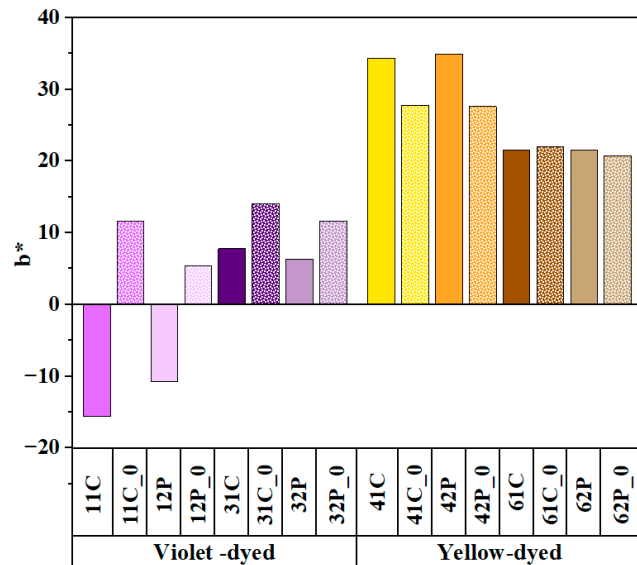
Before UV light exposure, the highest K/S was found in sample 11C, with the strongest violet color in a combination of red and blue hues. This is attributed to the aromatic ring (C=C) of phenyl groups in shikonin, which presumably contributed to the dye deposition on the cotton surface. The K/S values of 2.908 (11C) went downward to 1.749 (21C), followed by 0.716 (31C).

After being exposed to UV light, the most significant change in K/S was in the violet-dyed cotton samples without UV treatments. The highest K/S of sample 11C (2.908) drastically decreased to that of the untreated sample (0.695), indicating the untreated sample was the most powerfully faded. This severe color change after UV treatment can be attributed to the absence of carbon–carbon double bonds in cotton, which made the chromophores permanently attached to the cotton [48]. Compared with the violet-dyed fabrics, the yellow-dyed samples showed a gradual descent in K/S.



**Figure 6.** K/S values of natural-dyed, UV-treated cotton/polyester before and after the exposure to UV light.

To investigate the impacts of UV light exposure on the chromaticity, Figure 7 demonstrates the colorimetric parameter  $b^*$  values of the UV-treated fabrics. Of the utmost importance is that the UV treatments led to yellowing in the violet-dyed samples; however, the yellow dyeing did not significantly discolor the fabrics even after UV exposure. After exposure to UV light, the violet-dyed samples became less reddish and more yellowish. The UV-exposed samples in violet showed considerable increases in  $b^*$  values, showing the highest rise of the samples (11C and 11C<sub>0</sub>) from (−)15.71 to (+)11.54.



**Figure 7.** CIELAB  $b^*$  values of natural-dyed, UV-treated cotton/polyester before and after the exposure to UV light.

In contrast to the violet-dyed ones, the yellow-dyed samples did not change considerably because the yellow hues did not turn bluish greatly with a small decrease in  $b^*$  values (mean 28.838). The  $b^*$  values of the UV-exposed samples (61C, 62P) were almost identical to those of the unexposed ones. It can be inferred that non-photochemical xanthophyll allowed fluorescence quenching to detoxicate reactive oxygen and dissipate excessive photon energy [49]. The carotenoid chromophores did not fade fabrics much due to the

rapid equilibrium of isomerization and the excitation and oxidation of free radicals at low critical UV irradiation, despite other factors to consider [25,50].

With the impacts of two natural dyes on the chromaticity above, Table 3 expresses the color differences ( $\Delta E$ ) of the dyed fabrics between unexposed and UV-exposed fabrics. In this study, the  $\Delta E_{ab}$  was given from the UV-vis reflectance spectra using CIE1976 color space L a\*b\* coordinates, which were converted into L C\*h\* parameters to obtain the  $\Delta E^*_{00}$  from the CIE2000 formula with weighing factors [35]. These values were mathematically modified for the  $\Delta E^*_{cmc}$  of the color tolerance CMC system with quasimetric parameters. This was because theoretically calculated chromatic values are inconsistent with human perception; hence, it is necessary to minimize the inconsistency of  $\Delta E$  via various formulae, as suggested in several papers [37,38,51].

**Table 3.** Color difference of the violet- and yellow-dyed fabrics before and after exposure to UV light.

Sample	CIE1976 $\Delta E_{ab}$	CMC $\Delta E_{cmc}$ (2:1)	CIEDE2000 $\Delta E_{00}$	Mean $\Delta E \pm$ Std.
11C, 11C_0	37.03	27.51	25.00	29.85 $\pm$ 6.35
21C, 21C_0	32.64	26.15	21.46	26.75 $\pm$ 5.61
31C, 31C_0	6.60	8.70	22.57	12.62 $\pm$ 8.68
12P, 12P_0	24.82	18.65	21.59	21.69 $\pm$ 3.09
22P, 22P_0	22.26	18.26	21.61	20.71 $\pm$ 2.15
32P, 32P_0	6.22	7.92	18.65	10.93 $\pm$ 6.74
41C, 41C_0	7.49	3.35	18.01	9.62 $\pm$ 7.56
51C, 51C_0	7.98	3.74	4.79	5.50 $\pm$ 2.21
61C, 61C_0	2.60	1.13	5.95	3.23 $\pm$ 2.47
42P, 42P_0	8.16	3.63	18.66	10.15 $\pm$ 7.71
52P, 52P_0	4.46	2.22	2.90	3.19 $\pm$ 1.15
62P, 62P_0	1.60	1.06	2.44	1.70 $\pm$ 0.70

First, the color of violet-dyed samples changed much more substantially (mean  $\Delta E$ : 20.42) than that of the yellow-dyed ones (mean  $\Delta E$ : 5.57) after UV exposure, as already found in Figure 7. The biggest color difference was seen in the violet-dyed cotton untreated sample before and after UV light exposure, and the value of  $\Delta E$  ranged from 37.03 (CIE1976) to 27.51 (CMC l:c = 2:1) and 25.00 (CIEDE2000). The violet-dyed polyester samples generally discolored to a lesser extent (mean  $\Delta E$ : 17.78) than the cotton ones (mean  $\Delta E$ : 23.07) under the same conditions.

Second, the  $\Delta E$  narrowed down in the following order: the untreated samples > the ZnO-treated samples > the ZnO/polyphenol-treated samples. This tendency was the same as the  $\Delta E_{cmc}$  order of the violet cotton, the violet polyester, and the yellow polyester. The negligible exception was found in the yellow cotton between the untreated samples (3.35) and the ZnO-treated ones (3.63). The least color difference ( $\Delta E$  of 1.60) was seen in the ZnO/polyphenol-treated polyester (62P) in yellow dyeing. The average  $\Delta E$  of all three models stood out in the order of the pristine violet (29.85) > the ZnO-treated violet (26.75) > the ZnO/polyphenol-treated violet (12.62) > the pristine yellow (9.62) > the ZnO-treated yellow (5.50) > and the ZnO/polyphenol-treated yellow (3.23)-dyed cotton samples.

Third, the unexposed samples with the ZnO/polyphenol treatment did not differ from the UV-exposed ones. In Table 3, both ZnO/polyphenol-treated cotton and polyester in violet/yellow-dyeing samples had a very narrow range of color differences ( $\Delta E_{ab}$ : 6.60 and 6.22 in violet-dyeing, 2.60 and 1.60 in yellow-dyeing). The smallest  $\Delta E$  was found in the ZnO/polyphenol-treated polyester (62P and 62P\_0), the order of which stands as CIEDE2000  $\Delta E_{00}$  (2.44) > CIE1976  $\Delta E_{ab}$  (1.60) > CMC  $\Delta E_{cmc}$  (1.06). Notably, the color difference  $\Delta E_{00}$  in CIEDE2000 was distributed with an even deviation. In conclusion, despite the ZnO/phenol treatments lowering the K/S and chroma before UV exposure, the ZnO/phenol treatments caused the least color changes in both colored cotton and polyester fabrics after exposure to UV light.

Table 4 shows the reflectance rates of the dyed fabrics in the UVB range (at 294 nm). Overall, the ZnO-treated samples reflected more UV light than the untreated ones, in contrast to the ZnO/polyphenol-treated samples, which had higher UV absorption. In Table 4, the reflectance rates increased to 13.60% (21C) from 11.14% (11C) and to 13.01% (22P) from 5.57% (12P) after the ZnO treatment. This increase in reflectance was consistent with that of the cotton and polyester in yellow, which increased by 2.13% (41C–51C). On the contrary, the reflectance rates sharply decreased from 11.14% to 3.84% in the violet-dyed cotton (11C–31C) after the ZnO/polyphenol treatment. This can be attributed to the hydroxyl groups of polyphenolic tannin, which can cross-link other molecules with their (-OH) bonds to improve dye affinity [38]. When the tannin from gallnut reacted with the shikonin chromophores, the double-bond (C=C) aromatic rings from a phenolic compound could impart  $\pi$ -electron bonds to its carboxylic group, resulting in the improvement of UV absorption [52]. These findings can imply the effectiveness of the ZnO/phenol treatments in UV protection, despite their low color strength and chroma.

**Table 4.** Reflectance rates of the dyed cotton and polyester samples in UV-B (at 294 nm).

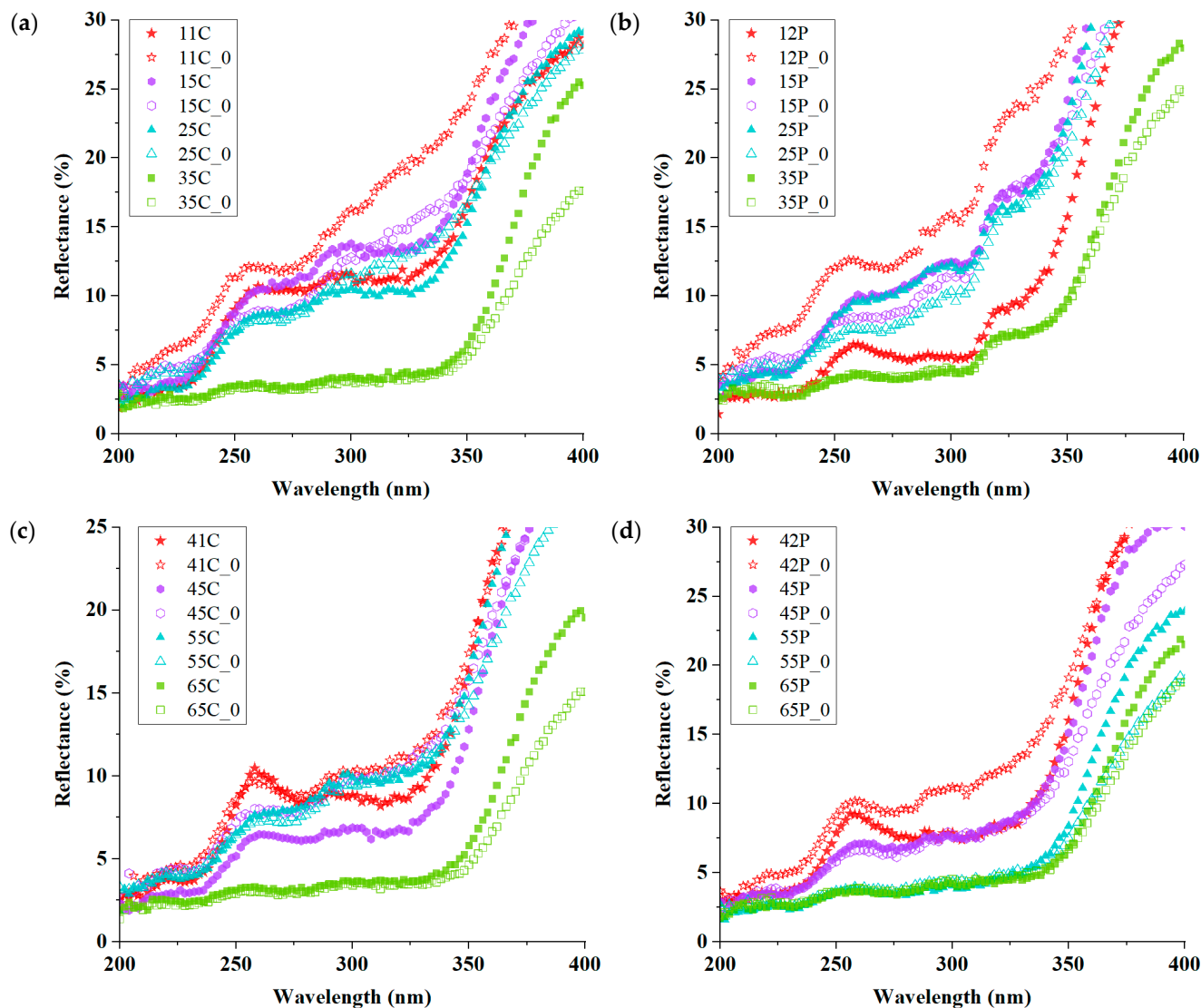
Violet-Dyed Sample	Reflectance (%)	Yellow-Dyed Sample	Reflectance (%)
11C	11.14	41C	8.81
21C	13.60	51C	10.94
31C	3.84	61C	3.70
12P	5.57	42P	7.43
22P	13.01	52P	7.57
32P	5.28	62P	3.69

### 3.5. Effects of Copper Acetate Mordants on UV Protection and Chromaticity

To conduct a closer examination of the UV photo-absorber, Figure 8 illustrates the effects of the Cu-mordants on the dyed samples in which the ZnO/polyphenol were treated. In Figure 8a–d, all the reflectance spectra go downward from UVA (400 to 315 nm) to UVB (315 to 280 nm) ranges, with the excitonic absorption peak at 258 nm. The most prominent point was found in the Cu-mordanted samples with ZnO/polyphenol treatment before and after UV exposure. After Cu-mordanting, the reflectance rates of the ZnO/polyphenol-treated samples were much lower than those of the untreated or the ZnO-treated ones in UV-B. It was found that the combination of Cu-mordanting with ZnO/polyphenol treatments made the fabrics less reflective, i.e., more absorbent than the unexposed samples in UV-A. The hydroxyl groups from tannin provided good affinity with other molecules, resulting from the formation of hydrogen bonds [53].

Cu-mordanting contributed to the narrowing of the gap between unexposed and UV-exposed samples. This phenomenon was predominant in the polyester fabrics dyed violet, as examined in Figure 8b. In contrast to the high gap between the pristine polyester of samples 12P and 12P\_0, the other Cu-mordanted samples after UV exposure showed almost identical reflectance to the unexposed samples. In Figure 8d, all Cu-mordanted polyester samples in yellow dyeing were less reflective and more absorptive than the unexposed ones without Cu-mordant. The Cu-mordants could prohibit the reoccurrence of electron deficiency due to the chemical reduction of oxide compounds by the transferred electron from the excited state by light absorption. During the photo-induced charge separation, the electron acceptor generates negative charges that could react with metal ions, thereby forming Cu-chelate ligands [13,14].





**Figure 8.** Reflectance curves of the violet-dyed (a) cotton and (b) polyester and the yellow-dyed (c) cotton and (d) polyester without/with Cu-mordant before/after UV light exposure in the UVA and UVB ranges.

The Cu-phenolic-chelating networks can impart the improvement in color strength and the fixation of UV absorbers to the ZnO/tannin-treated, Cu-mordanted, and dyed fabrics. Of importance, the color differences between yellow-dyed cotton and polyester were nearly zero, indicating that the UV exposure did not fade the 65C and 65P samples but rather turned them into improved chroma ( $C^*$ ), as found in Figure 9. However, the other samples seemed slightly faded, with lower chroma and changes in hue. UV light shielding can benefit from dyeing in darker hues or increasing the color depth ( $K/S$ ). When absorbing UV light, the yellow chromophores can transfer the excited electrons to acceptors, lose the electrons, and then generate positive holes and hydroxyl or hyper-oxidative groups, which damages the chromophores [54]. However, copper acetate mordanting enhanced the coloration of the ZnO/polyphenol-treated samples. This improvement could be attributed to the coordinate linkage of  $Cu^{2+}$  ions and carbonyl groups from the oxidation of phenols that were attached to the fabric surface, consistent with the previous study [55]. Consequently, Cu-mordanting with the ZnO/polyphenol-treatments could contribute to not just coloration by deepening color shades but also UV protection.

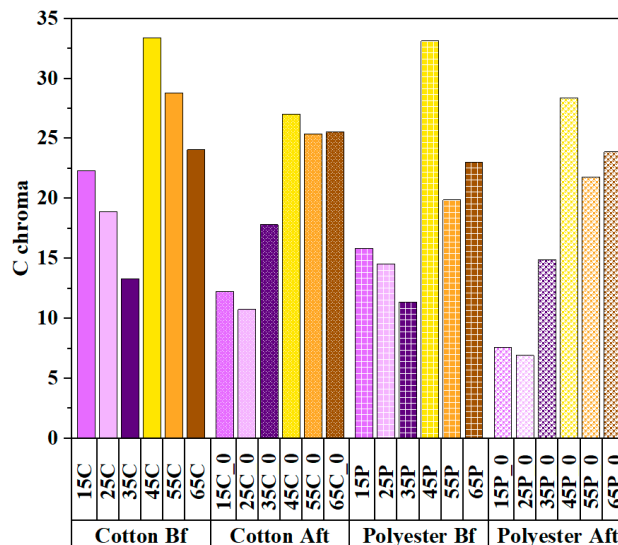


Figure 9. Chroma values of Cu-mordanted cotton and polyester before and after UV exposure.

In addition to the chroma values in Figure 9, Figure 10 exhibits the hue change in Cu-mordanted fabrics after UV exposure. The most important change was seen in the violet-dyed samples. The hue angles of the unexposed samples indicated the color of bluish violet, ranging from 315° to 317°. After the UV exposure, the hue angle shifted to reddish purple at approximately 50° to 68°. There was no significant difference between the cotton and polyester samples in hue values. To sum, the ZnO/polyphenol-treated sample with Cu-mordanting still kept its chroma and hue angles even better after UV exposure.

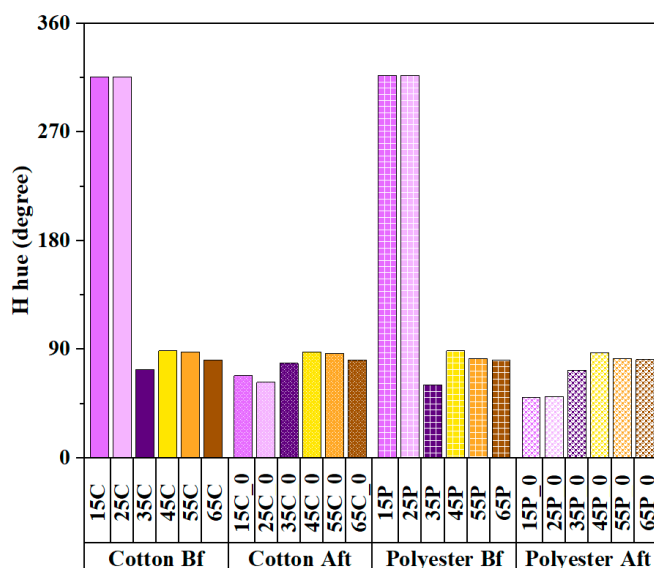


Figure 10. Hue angle values of Cu-mordanted cotton and polyester before and after UV exposure.

3.6. Effects of Copper Acetate Mordants on UV Protection and Chromaticity

To find the effectiveness of ZnO/polyphenol treatments, Table 5 compares the ΔE between the unexposed and the UV-exposed samples, which were Cu-mordanted via three colorimetric formulae. The highest color differences (mean: 25.90 ± 4.34) occurred in violet-dyeing and Cu-mordanting for the untreated cotton, followed by the untreated polyester (mean ΔE 16.03 ± 2.72). In other words, the ZnO/phenol treatments helped in the reduction in ΔE. In the presence of ZnO/polyphenol, the unexposed and UV-exposed samples with yellow-dyeing did not differ greatly from each other, showing a minute amount of ΔE 2.09 ± 1.03 (cotton) and 0.69 ± 0.30 (polyester), respectively. On the contrary,

the ZnO/polyphenol treatments drastically decreased the  $\Delta E$  from one-sixth to one-fourth in violet-dyed samples (mean: 4.42 to 4.43). In conclusion, it was articulated that the yellow-dyed fabrics that were Cu-post-mordanted and treated with ZnO/polyphenols were effective in increasing color similarity and decreasing color variation by UV light exposure.

**Table 5.** Comparisons in color differences ( $\Delta E$ ) between the unexposed and UV-exposed samples of Cu-mordanting with or without zinc oxide and polyphenol treatments.

Sample	CIE1976 $\Delta E_{ab}$	CMC $\Delta E_{cmc}$ (2:1)	CIEDE2000 $\Delta E_{00}$	Mean $\Delta E \pm$ Std.
15C, 15C_0	30.27	25.83	21.59	25.90 $\pm$ 4.34
15P, 15P_0	17.58	17.63	12.89	16.03 $\pm$ 2.72
35C, 35C_0	6.15	2.77	2.90	4.42 $\pm$ 1.64
35P, 35P_0	4.55	2.26	3.13	4.43 $\pm$ 1.24
45C, 45C_0	6.74	2.05	1.98	3.94 $\pm$ 2.49
45P, 45P_0	4.45	1.07	1.12	2.58 $\pm$ 1.70
65C, 65C_0	3.28	1.43	1.57	2.09 $\pm$ 1.03
65P, 65P_0	1.00	0.65	0.41	0.69 $\pm$ 0.30

To find the applicability of each dyed cotton or polyester fabric with ZnO/polyphenol treatments to practical uses, Table 6 indicates color fastness to light and washing. Overall, the samples demonstrated very good or excellent fastness to washing. Though the color fastness to light (xenon arc) was fair or good, it was much improved than that of the only-one-cycle-dyed samples without UV treatments or Cu-post mordanting (grade: 1–2, exposed to carbon arc). The violet-dyed UV treated fabrics with Cu-mordants revealed slightly higher grades (grade: 3–4) than those of the yellow-dyed fabrics (grade 3). This color change seemed dissimilar to the result in Table 5. This could be attributed to many reasons, such as the different wavelengths of artificial light between UV-C lamps in Table 5 and the xenon arc (similar to sunlight) in Table 6. In terms of the washing fastness, the resistance of color change by laundering at  $40 \pm 2$  °C was good (grade: 3 or 3–4). The resistance to color staining was very good or excellent among all the tested samples (grade: 4–5).

**Table 6.** Color fastness to light and color fastness to washing of the violet- and yellow-dyed cotton and polyester with ZnO/polyphenol treatments.

Sample	Color Fastness to Light	Color Fastness to Accelerated Washing			
		Change	Staining		
			Cotton	Wool	Polyester
35C	3–4	3	4–5	4–5	*
35P	3–4	3	4–5	*	4–5
65C	3	3–4	4–5	4–5	*
65P	3	3	4–5	*	4–5

The symbol (\*) indicates that the testing fabric in that column (wool/polyester) had not been subjected to color fastness testing to washing with the samples present in that row.

## 4. Discussion

### 4.1. Strategies for Improving Chromaticity for UV Shielding

To improve UV protection and prevent discoloration, this study suggests three strategies: (1) natural dyeing with *Cape jasmine* colorant; (2) ZnO/polyphenol treatment; and (3) Cu-post-mordanting. First, the xanthophyll chromophores in nature play a role in controlling the excessive number of chlorophyll chromophores that were produced by much more intensive photo-energy. In other words, the xanthophyll is a non-photochemical and is normally screened by the chlorophyll, yet it appears in the absence of the chlorophyll. In this work, this natural phenomenon was imitated for the purpose of UV light shielding. Second, ZnO, as a photo-absorber, has either positive or negative effects on light fastness

and photodegradation because of its redox-processability. Photodegradation efficiency may be accelerated by a high ZnO loading, but degradation can stabilize below a critical ZnO loading [19,54]. Additionally, polyphenolic tannic acid, as a bio-mordant, can fixate basic, cation, and reactive dyes onto fabric surfaces through the formation of covalent bonds with the dyes at pH levels that are controlled. The phenolic tannin, as an oxidant, can improve the light fastness of hydrophilic cotton fabrics by transforming photo-oxidative double bonds into photo-labile single bonds for the prevention of photodegradation. Third, inorganic mordants, as auxochromes, can improve the diffusion, adsorption, and fixation of dye molecules, leading to the formation of a coordination complex. Metallic salts such as sodium carbonate, sodium sulfate, aluminum potassium sulfate, copper sulfate, and iron sulfate are unable to colorize themselves due to their non-photo-absorbency, but they can help the chromophores deepen the color shade variation of fabrics.

#### 4.2. Limitation

There are some limitations to this research. The traditional procedures were used to process natural dyeing and mordanting. i.e., the dyeing parameters were already set, such as the concentration of dyes (the ratio of o.w.f.), the types of extract solvent, or the dyeing temperature. Second, the ZnO treatment was implemented after pre-mordanting and dyeing to prepare control samples for being pristine. The excessive amount of ZnO use could be detrimental to cell longevity, hydrogen peroxide production, and the ecosystem's photosynthesis of phytoplankton [17]. However, further experiments concerning cytotoxicity were not conducted in this study. Third, the material selection was limited by the exclusion of toxic, carcinogenic mordants such as chromium or azoic dyes. There have been continuous concerns about waste dyeing water for marine ecosystems in the textile industry; therefore, this study aimed at the minimum discharge of dyeing wastes following traditional preparation for dyeing and mordanting. After the experiments, the residue waste was collected as fertilizer.

#### 5. Conclusions

Despite the high-tech chemicals for UV protective functionalization, natural dyes with traditional metal mordants have come back to protect aquatic ecosystems from pollution. In this work, natural dyeing from *Gromwell red* roots and *Cape jasmine* seeds was used for the purpose of the UV-protective fabrics. The FTIR results confirmed that naphthoquinone (shikonin) and carotenoid (xanthophyll) chromophores, in the presence of carboxyl functional groups, derived the violet and yellow hues of the dyed fabrics. The dyed cotton and cotton/polyester were treated with ZnO and polyphenols before Cu-post mordanting. The ZnO nanoparticles (mean: 183.39 nm c-axis length, 131.87 nm basal edges) were seen on SEM, TEM, and XRD. They stuck to the fiber surfaces and twisted strands, which made the K/S values go down. The UV exposure led to a decrease in K/S for both kinds of color dyeing, while the color changes in CIELAB b\* values demonstrated an opposite trend, with violet dyeing showing an upward trend to positive (+) b\* values and yellow dyeing showing a downward trend. The UV-vis spectra showed that the ZnO made the material reflect more UVA and UVB light, while the polyphenolic tannin from gallnuts made it absorb more UV light. The Cu-mordants enhanced the fixation of colorants, thus resulting in a minimum  $\Delta E$  between the UV-exposed/unexposed samples. This fact also supported excellent color fastness to washing (4–5 grades) in color staining. Though the color fastness to light was fair, the light resistance of five cycles of dyeing with ZnO/phenol treatment and Cu mordants was much improved compared with only one cycle of dyeing without the treatment or mordants (3–4 grades from 1–2 grades). This study found the effectiveness of natural dyes, UV absorbers of ZnO/polyphenol, and Cu mordant in protecting skin from UV threats due to ozone depletion.

**Funding:** This research received no external funding.

**Institutional Review Board Statement:** Not applicable.

**Informed Consent Statement:** Not applicable.

**Data Availability Statement:** Restrictions apply to the availability of the photographs of *red-root Gromwell* plants, and *Cape jasmine* plants. Data were obtained from National Species Knowledge Information System and are available from Korea National Arboretum (photographer: Sooyoung Jeong) at [www.nature.go.kr](http://www.nature.go.kr) with the permission of Korea National Arboretum.

**Conflicts of Interest:** The author declares no conflict of interest.

## References

1. Ghazi, S. Do the polyphenolic compounds from natural products can protect the skin from ultraviolet rays? *Results Chem.* **2022**, *4*, 100428. [[CrossRef](#)]
2. Kouassi, M.C.; Grisel, M.; Gore, E. Multifunctional active ingredient-based delivery systems for skincare formulations: A review. *Colloids Surf. B Biointerfaces* **2022**, *217*, 112676. [[CrossRef](#)] [[PubMed](#)]
3. Qin, J.; Guo, N.; Yang, J.; Chen, Y. Recent Advances of Metal–Polyphenol Coordination Polymers for Biomedical Applications. *Biosensors* **2023**, *13*, 776. [[CrossRef](#)] [[PubMed](#)]
4. Salvo, D.E.; Gangemi, S.; Genovese, C.; Cicero, N.; Casciaro, M. Polyphenols from Mediterranean Plants: Biological Activities for Skin Photoprotection in Atopic Dermatitis, Psoriasis, and Chronic Urticaria. *Plants* **2023**, *12*, 3579. [[CrossRef](#)] [[PubMed](#)]
5. Du, H.; Yue, M.; Huang, X.; Duan, G.; Yang, Z.; Huang, W.; Yin, X. Preparation, application and enhancement dyeing properties of ZnO nanoparticles in silk fabrics dyed with natural dyes. *Nanomaterials* **2022**, *12*, 3953. [[CrossRef](#)] [[PubMed](#)]
6. Guan, W.; Zhang, L.; Wang, C.; Wang, Y. Theoretical and experimental investigations of the thermoelectric properties of Al-, Bi- and Sn-doped ZnO. *Mater. Sci. Semicond. Process.* **2017**, *66*, 247–252. [[CrossRef](#)]
7. Jacob, J.; Rehman, U.; Mahmood, K.; Ali, A.; Mehboob, K.; Ashfaq, A.; Ashraf, F. Improved thermoelectric performance of Al and Sn doped ZnO nano particles by the engineering of secondary phases. *Ceram. Int.* **2020**, *46*, 15013–15017. [[CrossRef](#)]
8. Otaviano, B.T.H.; Sannomiya, M.; de Lima, F.S.; Tangerina, M.M.P.; Tamayose, C.I.; Ferreira, M.J.P.; da Costa, S.M. Pomegranate peel extract and zinc oxide as a source of natural dye and functional material for textile fibers aiming for photoprotective properties. *Mater. Chem. Phys.* **2023**, *293*, 126766. [[CrossRef](#)]
9. Vittal, R.; Ho, K.C. Zinc oxide based dye-sensitized solar cells: A review. *Renew. Sustain. Energy Rev.* **2017**, *70*, 920–935. [[CrossRef](#)]
10. Belay, A.; Mekuria, M.; Adam, G. Incorporation of zinc oxide nanoparticles in cotton textiles for ultraviolet light protection and antibacterial activities. *Nanomater. Nanotechnol.* **2020**, *10*, 1847980420970052. [[CrossRef](#)]
11. Rise, M.S.; Ranjbar, A.H.; Noori, H.; Saheb, V. Synthesis and characterization of ZnO nanorods-Zn<sub>2</sub>SiO<sub>4</sub> nanoparticles-PMMA nanocomposites for UV-C protection. *Opt. Mater.* **2022**, *123*, 111922. [[CrossRef](#)]
12. Baranei, M.; Taheri, R.A.; Tirgar, M.; Saeidi, A.; Oroojalian, F.; Uzun, L.; Goodarzi, V. Anticancer effect of green tea extract (GTE)-Loaded pH-responsive niosome Coated with PEG against different cell lines. *Mater. Today Commun.* **2021**, *26*, 101751. [[CrossRef](#)]
13. Brza, M.A.; Aziz, B.A.; Anuar, F.; Dannoun, E.M.A.; Saeed, S.R.; Mohammed, S.J.; Abdulwahid, R.T. Green coordination chemistry as a novel approach to fabricate polymer:Cd(II)-complex composites: Structural and optical properties. *Opt. Mater.* **2021**, *116*, 111062. [[CrossRef](#)]
14. Feng, Y.; Li, P.; Wei, J. Engineering functional mesoporous materials from plant polyphenol based coordination polymers. *Coord. Chem. Rev.* **2022**, *468*, 214649. [[CrossRef](#)]
15. Fernandes, S.C.; Alonso-Varona, A.; Palomares, T.; Zubillaga, V.; Labidi, J.; Bulone, V. Exploiting mycosporines as natural molecular sunscreens for the fabrication of UV-absorbing green materials. *ACS Appl. Mater. Interfaces* **2015**, *7*, 16558–16564. [[CrossRef](#)] [[PubMed](#)]
16. Luo, J.; Liu, Y.; Yang, S.; Flourat, A.L.; Allais, F.; Han, K. Ultrafast barrierless photoisomerization and strong ultraviolet absorption of photoproducts in plant sunscreens. *J. Phys. Chem. Lett.* **2017**, *8*, 1025–1030. [[CrossRef](#)] [[PubMed](#)]
17. Sen, S.; Mallick, N. Mycosporine-like amino acids: Algal metabolites shaping the safety and sustainability profiles of commercial sunscreens. *Algal Res.* **2021**, *58*, 102425. [[CrossRef](#)]
18. He, Y.; Li, N.; Xiang, Z.; Rong, Y.; Zhu, L.; Huang, X. Natural polyphenol as radical inhibitors used for DLP-based 3D printing of photosensitive gels. *Mater. Today Commun.* **2022**, *33*, 104698. [[CrossRef](#)]
19. Groeneveld, I.; Kanelli, M.; Ariese, F.; van Bommel, M.R. Parameters that affect the photodegradation of dyes and pigments in solution and on substrate—An overview. *Dyes Pigm.* **2023**, *210*, 110999. [[CrossRef](#)]
20. Rader Bowers, L.M.; Schmidtke Sobek, S.J. Impact of medium and ambient environment on the photodegradation of carmine in solution and paints. *Dyes Pigm.* **2016**, *127*, 18–24. [[CrossRef](#)]
21. Michelin, C.; Hoffmann, N. Photosensitization and photocatalysis—Perspectives in organic synthesis. *ACS Catal.* **2018**, *8*, 12046–12055. [[CrossRef](#)]
22. Abiola, T.T.; Whittock, A.L.; Stavros, V.G. Unravelling the photoprotective mechanisms of nature-inspired ultraviolet filters using ultrafast spectroscopy. *Molecules* **2020**, *25*, 3945. [[CrossRef](#)] [[PubMed](#)]
23. Deniz, N.G.; Iscan, A.; Sayil, C.; Avinc, O.; Kalayci, E. Naphthoquinone disperse dyes and their dyeing application to polyethylene terephthalate fabrics. *J. Text. Inst.* **2023**, 1–15. [[CrossRef](#)]

24. Dulo, B.; Phan, K.; Githaiga, J. Natural Quinone Dyes: A Review on Structure, Extraction Techniques, Analysis and Application Potential. *Waste Biomass Valorization* **2021**, *12*, 6339–6374. [CrossRef]
25. La, E.H.; Giusti, M.M. Ultraviolet–Visible Excitation of cis-and trans-pC coumaric Acylated Delphinidins and Their Resulting Photochromic Characteristics. *ACS Food Sci. Technol.* **2022**, *2*, 878–887. [CrossRef]
26. Maoka, T. Carotenoids as natural functional pigments. *J. Nat. Med.* **2020**, *74*, 1–16. [CrossRef] [PubMed]
27. Rafiq, A.; Ikram, M.; Ali, S.; Niaz, F.; Khan, M.; Khan, Q.; Maqbool, M. Photocatalytic degradation of dyes using semiconductor photocatalysts to clean industrial water pollution. *Ind. Eng. Chem. Res.* **2021**, *97*, 111–128. [CrossRef]
28. Canopoli, L.; Coulon, F.; Wagland, S.T. Degradation of excavated polyethylene and polypropylene waste from landfill. *Sci. Total Environ.* **2020**, *698*, 134125. [CrossRef] [PubMed]
29. Wang, X.; Sun, X.; Guan, X.; Wang, Y.; Chen, X.; Liu, X. Tannic interfacial linkage within ZnO-loaded fabrics for durable UV-blocking applications. *Appl. Surf. Sci.* **2021**, *568*, 150960. [CrossRef]
30. National Species Knowledge Information System, from Korea National Arboretum (Photographer: Sooyoung Jeong). Available online: [www.nature.go.kr](http://www.nature.go.kr) (accessed on 30 May 2024).
31. *ISO 105-B02*; Textiles—Tests for Colour Fastness—Part B02: Colour Fastness to Artificial Light: Xenon Arc Fading Lamp Test. ISO: Geneva, Switzerland, 2014.
32. *ISO 105-C06*; Textiles—Tests for Colour Fastness—Part C06: Colour Fastness to Domestic and Commercial Laundering. ISO: Geneva, Switzerland, 2010.
33. Ayesha, B.; Jabeen, U.; Naeem, A.; Kasi, P.; Malghani, M.N.K.; Khan, S.U.; Aamir, M. Synthesis of zinc stannate nanoparticles by sol-gel method for photocatalysis of commercial dyes. *Results Chem.* **2020**, *2*, 100023. [CrossRef]
34. Watkins, K. Online Tutorial: Using Excel to Calculate Hue Angles for CIE Lab Colour Space. Available online: <https://www.youtube.com/watch?v=2v-YuwVntFA> (accessed on 6 March 2024).
35. Bruce Lindbloom. Available online: [www.brucelindbloom.com](http://www.brucelindbloom.com) (accessed on 19 February 2024).
36. Wang, X.; Jiang, Y.; Du, J.; Xu, C. Establishment of a color tolerance for yarn-dyed fabrics from different color-depth yarns. *Color Res. Appl.* **2022**, *47*, 225–235. [CrossRef]
37. He, R.; Xiao, K.; Pointer, M.; Melgosa, M.; Bressler, Y. Optimizing Parametric Factors in CIELAB and CIEDE2000 Color-Difference Formulas for 3D-Printed Spherical Objects. *Materials* **2022**, *15*, 4055. [CrossRef] [PubMed]
38. Repon, M.R.; Dev, B.; Rahman, M.A.; Jurkonienė, S.; Haji, A.; Alim, M.A.; Kumpikaitė, E. Textile dyeing using natural mordants and dyes: A review. *Environ. Chem. Lett.* **2024**, *22*, 1473–1520. [CrossRef]
39. An, N.; Hu, J.; Ding, Y.; Sheng, P.; Zhang, Z.; Guo, X. Ionic liquid treated cellulose-based intelligent pH-responsive color indicator film, with excellent anti-ultraviolet function. *J. Polym. Res.* **2023**, *30*, 343. [CrossRef]
40. Soosairaj, A.; Pabba, D.P.; Gunasekaran, A.; Anandan, S.; Selvaraj, J.; Asirvartham, L.R. Synergetic impact of natural light harvesting materials to reduce the recombination rate and improve the device performance of dye sensitized solar cells. *J. Mater. Sci. Mater. Electron.* **2023**, *34*, 1748. [CrossRef]
41. Sun, Q.; Gong, T.; Liu, M.; Ren, S.; Yang, H.; Zeng, S.; Xu, H. Shikonin, a naphthalene ingredient: Therapeutic actions, pharmacokinetics, toxicology, clinical trials and pharmaceutical researches. *Phytomedicine* **2022**, *94*, 153805. [CrossRef] [PubMed]
42. Jeyaram, S. Spectral, third-order nonlinear optical and optical switching behavior of  $\beta$ -carotenoid extracted from phyllanthus niruri. *Ind. J. Phys.* **2022**, *96*, 1655–1661. [CrossRef]
43. Lin, P.; Chen, L.; Huang, X.; Xiao, F.; Fu, L.; Jing, D.; Wu, Y. Structural characteristics of polysaccharide GP2a in *Gardenia jasminoides* and Its Immunomodulatory Effect on Macrophages. *Int. J. Mol. Sci.* **2022**, *23*, 11279. [CrossRef] [PubMed]
44. Adedokun, O.; Adedeji, O.L.; Bello, I.T.; Awodele, M.K.; Awodugba, A.O. Fruit peels pigment extracts as a photosensitizer in ZnO-based Dye-Sensitized Solar Cells. *Chem. Phys.* **2021**, *3*, 100039. [CrossRef]
45. Saravanakumar, K.; Chelliah, R.; Shanmugam, S.; Varukattu, N.B.; Oh, D.H.; Kathiresan, K.; Wang, M.H. Green synthesis and characterization of biologically active nanosilver from seed extract of *Gardenia jasminoides* Ellis. *J. Photochem. Photobiol. B* **2018**, *185*, 126–135. [CrossRef]
46. Lee, J.; Kang, M.H.; Lee, K.B.; Lee, Y. Characterization of natural dyes and traditional Korean silk fabric by surface analytical techniques. *Materials* **2013**, *6*, 2007–2025. [CrossRef]
47. Guo, C.; He, J.; Song, X.; Tan, L.; Wang, M.; Jiang, P.; Peng, C. Pharmacological properties and derivatives of shikonin—A review in recent years. *Pharmacol. Res. Commun.* **2019**, *149*, 104463. [CrossRef] [PubMed]
48. Silva, P.M.D.S.; Fiaschitello, T.R.; Queiroz, R.S.D.; Freeman, H.S.; Costa, S.A.D.; Leo, P.; Costa, S.M.D. Natural dye from *Croton urucurana* Baill. bark: Extraction, physicochemical characterization, textile dyeing and color fastness properties. *Dyes Pigm.* **2020**, *173*, 107953. [CrossRef]
49. Liman, M.L.R.; Islam, M.T.; Repon, M.R.; Hossain, M.M.; Sarker, P. Comparative dyeing behavior and UV protective characteristics of cotton fabric treated with polyphenols enriched banana and watermelon biowaste. *Sustain. Chem. Pharm.* **2021**, *21*, 100417. [CrossRef]
50. Badmus, U.O.; Ač, A.; Klem, K.; Urban, O.; Jansen, M.A. A meta-analysis of the effects of UV radiation on the plant carotenoid pool. *Plant Physiol. Biochem.* **2022**, *183*, 36–45. [CrossRef] [PubMed]
51. Jiang, H.; Hu, X.; Khan, A.; Yao, J.; Tahir Hussain, M. Dyeing mechanism and photodegradation kinetics of gardenia yellow natural colorant. *Text. Res. J.* **2021**, *91*, 839–850. [CrossRef]
52. Seymour, J. Color inconstancy in CIELAB: A red herring? *Color Res. Appl.* **2022**, *47*, 900–919. [CrossRef]

53. Wulansari, A.D.; Hayati, D.; Long, D.X.; Choi, K.; Hong, J. Hydroxycinnamic acid derivatives for UV-selective and visibly transparent dye-sensitized solar cells. *Sci. Rep.* **2023**, *13*, 3235. [[CrossRef](#)]
54. Amir, M.; Ahmed, K.; Hasany, S.F.; Butt, R.A. Non-Covalent Bonding of Green Synthesized Copper Nanoparticles to enhance Physicochemical behavior of Sulfur-Dyed Cotton Fabric. *AATCC J. Res.* **2023**. [[CrossRef](#)]
55. Baldwin, A.; Booth, B.W. Biomedical applications of tannic acid. *J. Biomater. Appl.* **2022**, *36*, 1503–1523. [[CrossRef](#)]

**Disclaimer/Publisher's Note:** The statements, opinions and data contained in all publications are solely those of the individual author(s) and contributor(s) and not of MDPI and/or the editor(s). MDPI and/or the editor(s) disclaim responsibility for any injury to people or property resulting from any ideas, methods, instructions or products referred to in the content.